TELEDYNE SCIENTIFIC COMPANY
A Teledyne Technologies Company

Reducing Fracture Tendencies in PCBN FSW Tools

ONR Contract Number N00014-09-C-0288

Base Effort Final Report

Period: 2/3/2009 through 7/25/2010

Prepared for:
Dr. W. Mullins and Dr. J. DeLoach
ONR Code 332
Office of Naval Research
875 North Randal St
Arlington, VA 22203-1995

Prepared by:
David Marshall
Teledyne Scientific Co. LLC
1049 Camino Dos Rios
Thousand Oaks, CA 91360

Signed: D. B. Marshall

D. B. Marshall

REPORT DOCUMENTATION PAGE

Form Approved
OMB No. 0704-0188

PLEASE DO NOT RETURN YOUR FORM TO THE ABOVE ADDRESS.

1. REPORT DATE *(DD-MM-YYYY)*	2. REPORT TYPE	3. DATES COVERED *(From - To)*
7/25/2010	Base Effort Final Report	2/3/2009 to 7/25/2010

4. TITLE AND SUBTITLE

Reducing Fracture Tendencies in PCBN FSW Tools

5a. CONTRACT NUMBER

N00014-09-C-0288

5b. GRANT NUMBER

5c. PROGRAM ELEMENT NUMBER

6. AUTHOR(S)

David Marshall

5d. PROJECT NUMBER

5e. TASK NUMBER

5f. WORK UNIT NUMBER

7. PERFORMING ORGANIZATION NAME(S) AND ADDRESS(ES)

Teledyne Scientific Company
1049 Camino Dos Rios
Thousand Oaks, CA 91360

8. PERFORMING ORGANIZATION REPORT NUMBER

9. SPONSORING/MONITORING AGENCY NAME(S) AND ADDRESS(ES)

Dr. W. Mullins and Dr. J. DeLoach
ONR Code 332
Office of Naval Research
875 North Randal St
Arlington, VA 22203-1995

10. SPONSOR/MONITOR'S ACRONYM(S)

11. SPONSOR/MONITOR'S REPORT NUMBER(S)

12. DISTRIBUTION/AVAILABILITY STATEMENT

DISTRIBUTION A. Approved for public release; distribution is unlimited.

13. SUPPLEMENTARY NOTES

14. ABSTRACT

The overall goal of this program is to increase the life of PCBN tools in friction-stir welding of high temperature metals through understanding of mechanisms of damage development in the tool materials, identifying microstructural characteristics that mitigate this damage, and developing methods for measuring relevant material properties. Some key results from the first year of study are : (i) demonstration that cracking by indentation with a Vickers indenter can be used to obtain valid fracture toughness measurements in this class of materials ; (ii) some of the best performing materials were found to contain well dispersed diamond grains, a result that was unexpected by the manufacturers, (iii) An SEM imaging method was discovered that reveals internal deformation structures in BN grains, which are not normally detectable by SEM (useful for assessing damage caused by grain-to-grain contact during high pressure consolidation), (iv) observations from tools fractured during FSW indicate that crack growth occurs incrementally, likely over many thermal and/or mechanical cycles, rather than by unstable growth at a critical condition.

15. SUBJECT TERMS

Polycrystalline cubic boron nitride, Fracture toughness, microstructure, damage, friction-stir welding tools

16. SECURITY CLASSIFICATION OF:			17. LIMITATION OF ABSTRACT	18. NUMBER OF PAGES	19a. NAME OF RESPONSIBLE PERSON
a. REPORT	b. ABSTRACT	c. THIS PAGE			Dr. W. Mullins
					19b. TELEPHONE NUMBER *(Include area code)*

Contract Information

Contract Number	N00014-09-C-0288
Title of Research	Reducing Fracture Tendencies in PCBN FSW Tools
Principal Investigator	David Marshall
Organization	Teledyne Scientific Company

Technical Section

Technical Objectives

The overall goal of this program is to increase the life of PCBN tools in friction-stir welding of high temperature metals. This will be achieved through the following objectives:

(1) Understand the fundamental causes for limited lifetimes of PCBN tools during Friction-Stir Welding (FSW) of high temperature metals, including both wear and fracture.

(2) Identify microstructural characteristics and defects in PCBN materials that affect lifetime in FSW.

(3) Identify and develop simple mechanical/fracture test methods that can be used on PCBN materials as indicators of potential lifetime in FSW.

(4) Use information gained in (1) to (3) to guide development of new grades of PCBN or modifications to existing grades or tool design to improve lifetime during FSW.

Technical Approach

We have formed a multidisciplinary team to tackle the problem of increasing the life of PCBN tools in FSW of high temperature metals. Studies in this program at Teledyne Scientific are being coordinated with complementary, collaborative studies on manufacturing improved grades of PCBN at Megadiamond, tool manufacture at Advanced Metal Products, and other ONR supported FSW studies at Brigham Young University.

Two routes are being followed to improve tool life. One involves development of improved PCBN materials with increased resistance to damage. The other involves improvement of tool designs and control of FSW operating parameters to minimize detrimental loads on the tool during welding. Progress along both of these routes is currently impeded by gaps in our understanding of how damage (fracture and wear) develops in the tools during FSW, knowledge of the microstructural features or defects within the PCBN material that control the resistance to damage, and the capability to measure the relevant material properties that characterize the resistance to damage. The following studies are being undertaken in this program to fill these gaps:

(i) Identification of modes of failure and life-limiting damage during FSW by analysis of crack patterns in tools after being used in friction stir experiments, including: sectioning partly cracked tools to allow observation of fracture surfaces and to determine sub-surface crack shapes; monitoring crack development in interrupted tests; correlation of observed crack geometry with known thermal and mechanical stresses; and development of analytical fracture models to aid in distinguishing characteristics of stress distributions (static and cyclic) capable of giving the observed cracking behavior.

(ii) development of methods based on indentation fracture to measure fracture toughness, resistance to fatigue cracking, and resistance to thermal shock of PCNB materials, and to assess wear properties. Conventional fracture mechanics methods based on large test specimens are impractical with these

materials because they are only manufactured in small sizes (< 1 in^3), are extremely costly, and are extremely difficult to machine into test specimens.
(iii) Using a set of materials that show large differences in wear and cracking behavior during FSW, measure fracture properties, microstructural characteristics, and other relevant properties; then correlate these properties with FSW performance. These results will allow us to infer the influences of microstructure on toughness and other properties and thence on tool performance, as well as predict directions for modifying processing to improve tool life.

Progress Statement Summary

1. Identification of relations between tool life, microstructure, and toughness measurements. Initial experiments focused on materials from three lots of MS80 PCBN materials that showed large differences in properties. All consist of 80% BN, with the remainder mainly AlN, although the methods of powder mixing during processing differed. Two of these were used in FSW experiments and showed different susceptibility to cracking: one survived 206 plunges (#1298), whereas the other survived only two plunges (#1307). The third material, from a recent production run with modified heat treatment conditions, was found to be much more difficult to grind than the other two materials. We developed modified methods for polishing these three materials and demonstrated that cracking by indentation with a Vickers indenter can be used to obtain valid fracture toughness measurements. These measurements indicated that the fracture toughness of the new material that is difficult to machine was significantly higher than the toughnesses of the other two materials.

Microstructural analysis by scanning electron microscopy and Raman microprobe spectroscopy revealed that, surprisingly, the new material contained a significant amount of well dispersed diamond. The diamond particles are not expected to influence the indentation toughness measurements, although they clearly have an influence on the grinding and polishing behavior (and hence on tool wear). A detailed study was undertaken of the diamond impurities by EDS mapping at both TSC and Megadiamond. The study at Megadiamond included fracture surfaces and the BN powders that were used to fabricate the material. The latter indicated the presence of several possible impurity phases: diamond, B_4C, BC_2N, BC_4N, superhard B_6O, or C-BN solid solutions. The results suggest that sintering may promote reactions that redistribute and homogenize some compositions. The study at TSC identified peak overlap effects in EDS mapping that can give misleading indications of the diamond impurity compositions.
Following the discovery of these impurities, Megadiamond have initiated discussions with the vendor and implemented new powder qualification and tracking procedures

In the course of SEM examination of these and other materials we discovered (in collaboration with Megadiamond) an imaging method that reveals internal deformation structures in BN grains, which are not normally detectable by SEM. The method is useful for assessing damage caused by grain-to-grain contact during high pressure consolidation.

2. Understanding Fracture Causes and Mechanisms in PCBN: FSW tools with varying degrees of damage from FSW experiments were supplied by C. Sorensen and M. Mahoney at BYU. Several of the tool material inserts were removed from the tool holders for sectioning and fractography, with the aim of determining the sites of crack initiation. The observations indicate that crack growth occurs incrementally, likely over many thermal and/or mechanical cycles, rather than by unstable growth at a critical condition. Liquid Al was found filling the cracks in one tool, indicating that during FSW, temperatures throughout the tool exceeded the decomposition temperature of AlB_2 (~1,000^oC), which is formed in trace amounts in the grain boundary phase during densification. Under these conditions diffusion of Fe from the work piece occurred into the Al liquid in cracks through most of tool thickness.

Experiments are under way to observe the initiation and incremental growth of cracks during FSW. These experiments involve introducing controlled microcracks by loading a Vickers diamond indenter at various predetermined locations on the front, side and back surfaces of a tool insert, mounting the insert into a tool, and running interrupted FSW tests with periodic observations of crack initiation and growth at the insert surface, followed by sectioning and/or fracture at the end of the test to assess internal crack growth.

Progress

Fracture toughness measurement

The fracture toughnesses of the three MS80 materials described above were measured by indentation fracture. The method, which is summarized in Fig. 1, involves loading a Vickers diamond indenter on a polished surface, generating a contact zone of plastic deformation (from which the hardness can be evaluated) and two half-penny cracks centered on the indentation and aligned normal to the surface along the indentation diagonals. A fracture mechanics analysis of the formation of these cracks gives the expression in Fig. 1b, which is valid if the cracks are sufficiently large compared with the contact zone. This expression can be used to evaluate the fracture toughness from the measured crack lengths.

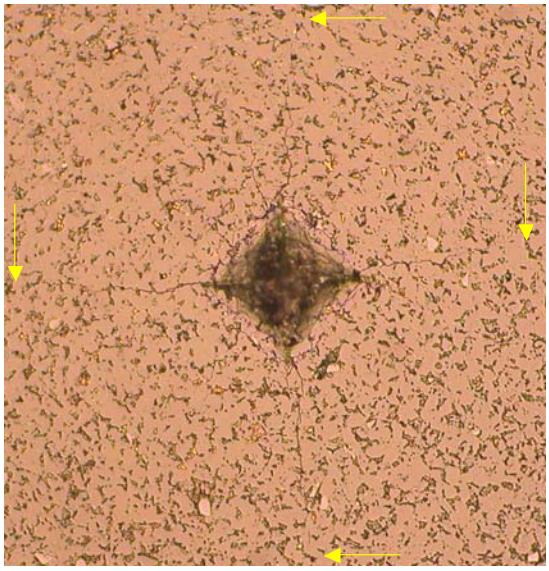

(a)

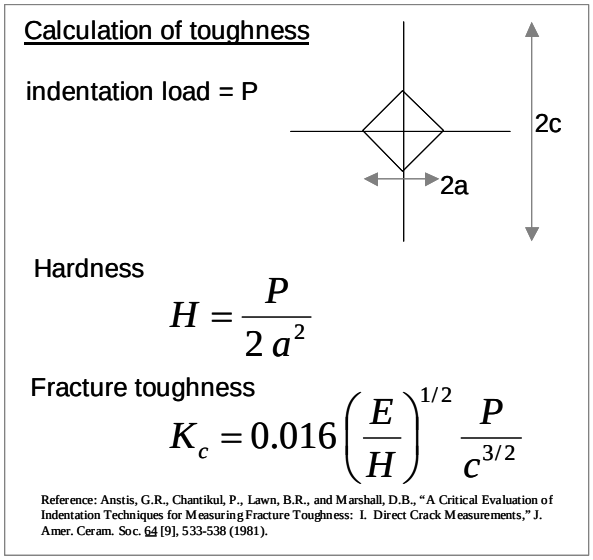

(b)

Fig. 1. Indentation method for measurement of fracture toughness: (a) Vickers indentation (200N load) in polished surface of polycrystalline cubic BN (MS80). Arrows indicate positions of crack tips, which can be readily located in higher magnification optical micrographs; (b) Schematic of indentation and cracks, with fracture mechanics expression from which the fracture toughness can be evaluated.

This technique has been developed extensively with ceramic materials, although it has not been applied previously to PCBN materials. Indentations in PCBN at loads smaller than ~50 N generally produce irregular crack patterns because of their high hardness and relatively large grain size. However, at higher loads well developed cracks are produced, as in Fig. 1.

One of the challenges in applying the method to these materials was in developing a method for locating the positions of the crack tips reliably. Initially, using surfaces that were not well polished, we found that optical microscopy was inadequate and high resolution electron microscopy was necessary, making the method extremely laborious. However, after developing an improved polishing method, we found that the crack tips could be located reliably using high magnification optical microscopy.

The results of toughness measurements from the three MS80 materials are summarized in Fig. 2. Also shown are measurements from another PCBN material (MN100) which has much higher volume fraction of BN and smaller amount of grain boundary phase (AlN). For each material the toughness was evaluated from indentations at several different loads within the range 50 to 200 N, with each data point being an average of at least 10 measurements. The observation in Fig. 2 that, in all cases, the toughness is independent of the indentation load confirms the functional form of the toughness equation and thus the validity of the underlying fracture mechanics analysis.

Significant differences are evident in the fracture toughnesses of the three MS80 materials. The highest toughness (5.2 MPa.m$^{1/2}$) is observed in the new material which was also much more difficult to grind and polish than the other two materials. However, the relative ranking for the other two materials is opposite to their relative performance in FSW: the material with lower toughness (#1298) is the one with the longer FSW life. Further measurements will be made to investigate whether this trend is followed in other materials.

The hardness of these materials is expected to scale with the volume fraction of BN and be relatively insensitive to subtle microstructural variations that influence fracture toughness. The measured hardnesses listed in Fig. 2 are consistent with this expectation: the values for the three MS80 materials are indistinguishable (30 GPa) whereas the value for the MN100 material is higher (34 GPa).

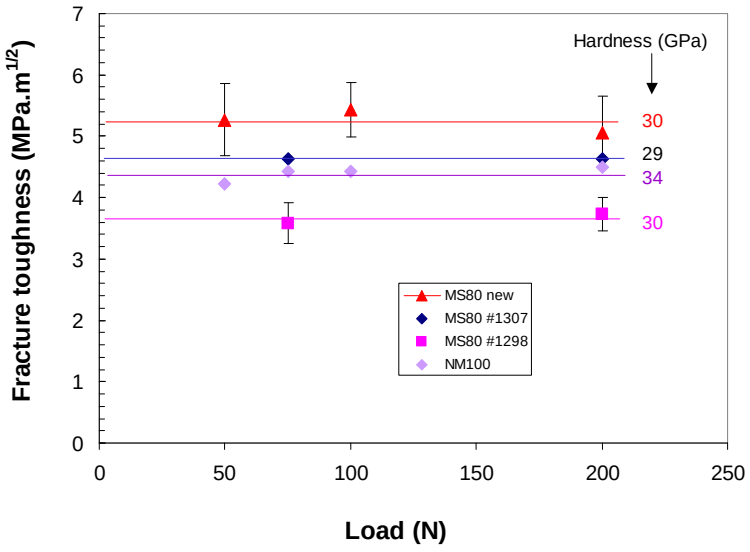

Fig. 2. Indentation fracture toughness measurements from several PCBN materials. Error bars indicate standard deviations.

Microstructural Analysis

Identification of diamond particles in new MS80 material

The new MS80 material was much more difficult to cut and polish than other PCBN materials. After initial attempts to polish the surface of this material using a relatively soft cloth that produced a good polish on other PCBN materials, we found that strong relief was produced, with some grains remaining raised significantly above the majority of grains. Images of these grains are shown in Fig. 3. EDS analysis indicated that these grains were carbon. Analysis by Raman microprobe spectroscopy confirmed that the grains are diamond (Fig. 4). The diamond grains were distributed very uniformly throughout the material, with a volume fraction of several percent. Their size is similar to that of the BN grains.

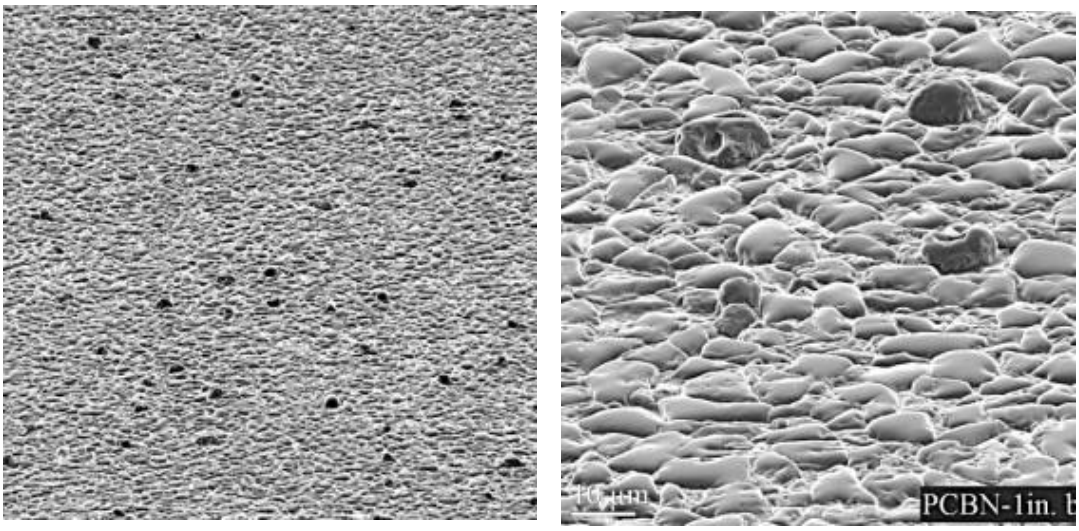

Fig. 3 SEM micrographs of new MS80 material showing surface after polishing with diamond impregnated cloth which produced relief of diamond particles (same area at different magnifications). Dark grains in (a) are diamond

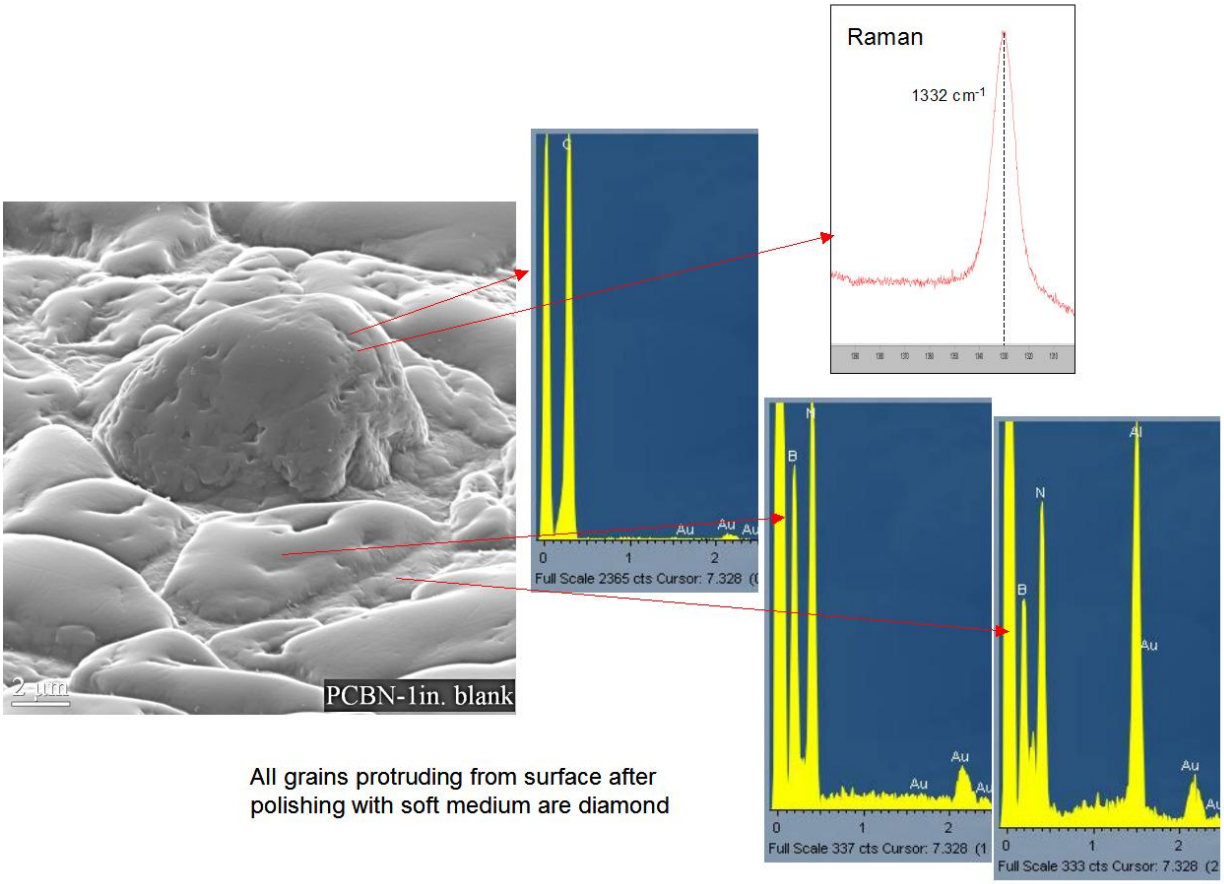

Fig. 4. SEM, EDS and Raman spectroscopy of diamond grains in new MS80 material

EDS mapping was carried out to assess whether other impurities were present. Typical results are shown in Fig. 5. The results showed a one-to-one correlation between grains showing large surface relief after polishing and carbon composition, indicating that the diamond grains were the only significant impurities. The remainder of the material consisted of BN grains with an AlN grain boundary phase, as expected. The oxygen map shows slightly higher oxygen concentration in the diamond particles than in the remainder of the material. However, we note that this map has been enhanced for visibility: the true intensities of the O signals are orders of magnitude lower than the B, N, and C signals.

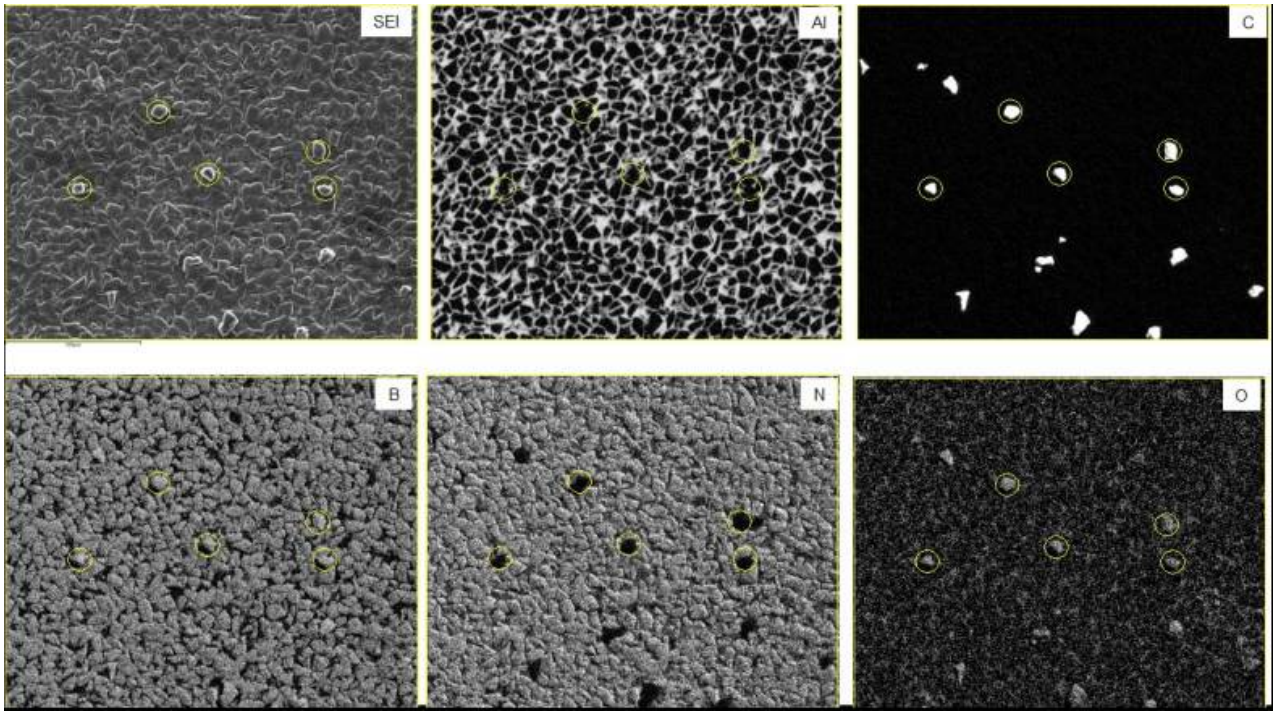

Fig. 5. EDS maps from polished surface of new MS80 material (yellow circles are references for fixed positions)

The boron map was at first sight puzzling, with the C grains showing a B signal with intensity slightly higher than the intensity of the B signal from the BN grains. However, this was shown to be an artifact due to finite width of the carbon peak and overlap with the position of the boron peak. EDS spectra from diamond and BN grains are shown in Fig. 6, with positions of B, N, and C peaks marked. The carbon peak from the diamond grain is slightly asymmetric, with intensity at the boron position approximately 10% to 15% of the peak value. The absolute intensity at this position is approximately the same as the absolute intensity of the boron peak from the BN grain, consistent with the EDS map (note the intensity scales for the diamond and BN grains in Fig. 5 differ by a factor of ~8). An EDS spectrum from a high purity graphite standard is shown in for comparison in Fig, 6. The carbon peak has shape and width identical to that from the diamond grain, thus confirming that the asymmetry of the carbon peak is due to an instrument characteristic and not due to overlap with a genuine boron peak.

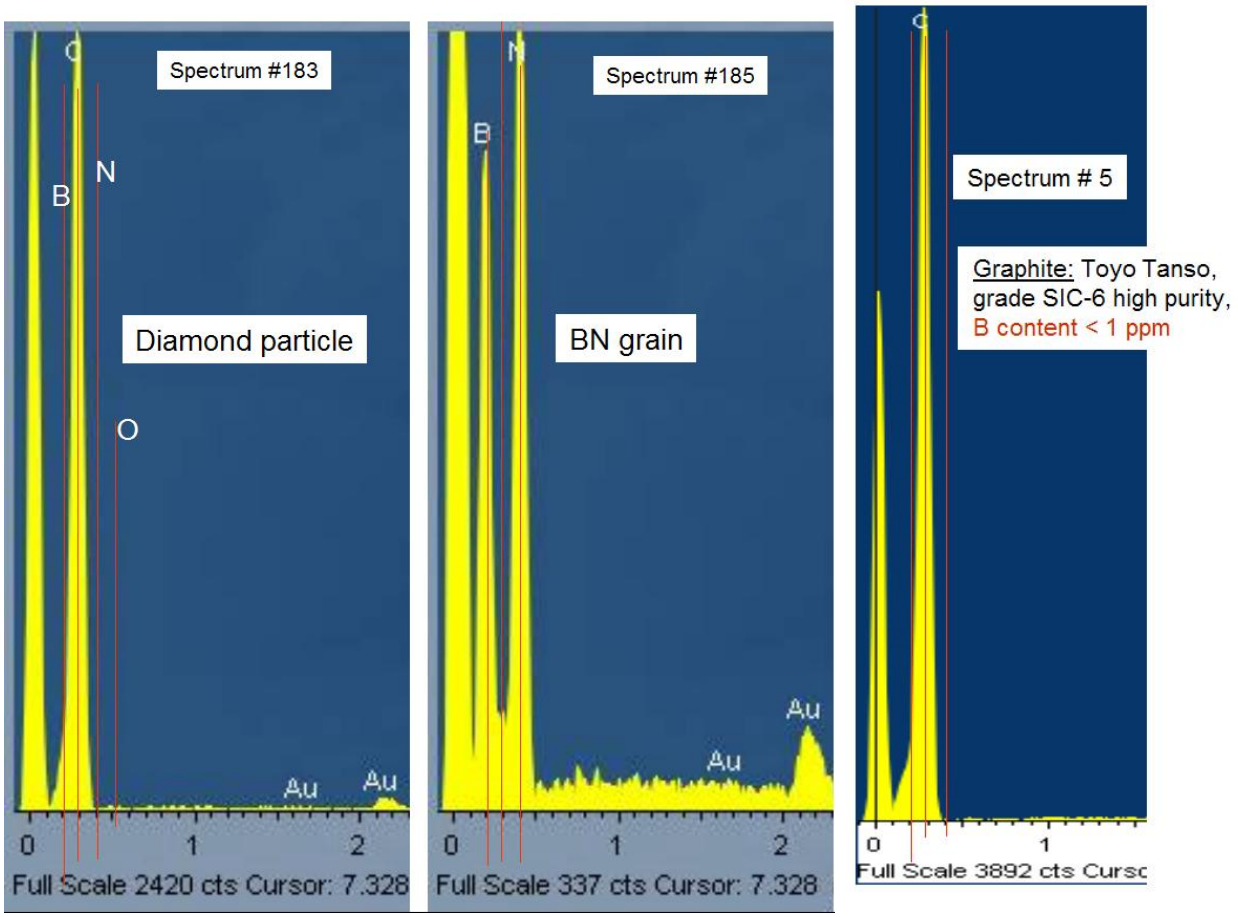

Fig. 6. Comparison of EDS spectra from diamond and BN grains in new MS80 and high purity graphite standard.

The spacing of the diamond grains is sufficiently large that very few were intersected by the indentation cracks used to measure the fracture toughness. Therefore, we do not expect the presence of the diamond grains to affect the fracture toughness. Similarly, the volume fraction of diamond is sufficiently small that a significant effect on hardness is not expected, consistent with the measurements summarized in Fig. 2. However, the presence of diamond grains may be expected to play a key role in increasing the resistance to grinding and polishing, as well as tool wear.

Imaging of internal deformation structures in BN grains

In the course of SEM examination of these materials we discovered (in collaboration with Megadiamond) an imaging method that reveals internal crystallographic structures in BN grains, which are not normally detectable by SEM. An example is shown in Fig 7. When imaged with secondary electrons, with a thin conducting layer of gold deposited on the surface to prevent charging (the usual procedure for insulating materials), the BN grains are featureless and the AlN grain boundary phase shows lighter contrast (Fig. 7a). Similar contrast is seen in backscattered electron images (Fig. 9). However, when imaged with secondary electrons without a conducting layer on the surface, dramatically different contrast is observed (Fig. 7b): crystallographic features resembling twins are clearly evident, more contrast detail is visible within the grain boundary phases, and there is a general reversal of contrast between the grains and the

grain boundary phase (the BN grains being lighter than the grain boundary phase). In many grains, there is a one-to-one correspondence between these crystallographic features and lines of surface relief visible by Nomarski interference (Fig. 7c). The surface relief may result from different polishing rates in regions of different crystallographic orientations.

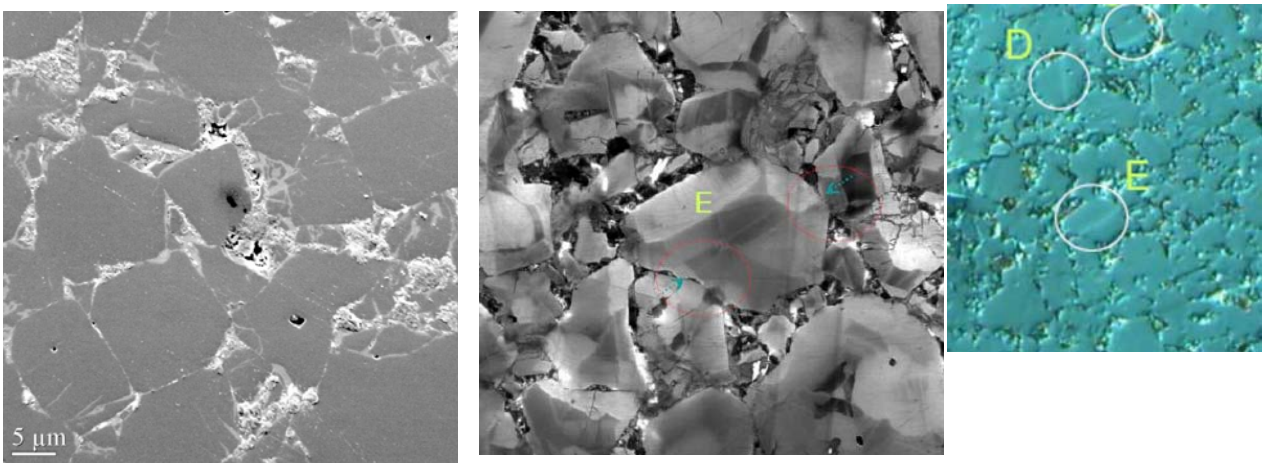

(a) (b) (c)

Fig. 7. Polished surface of MN100 material: (a) SEM image from surface coated with conducting layer of gold; (b) SEM image from uncoated surface (micrograph from Qingyuan Liu, Megadiamond); (c) Nomarski interference micrograph from area in (b), showing surface relief features in some grains.

The detailed contrast in images such as Fig. 7b was found to be sensitive to the accelerating voltage, with reversals of contrast occurring within some grains when the voltage was changed (Fig. 8). This and the observation that the contrast within the BN grains disappears when surface is coated with conducting gold suggests that contrast may be associated with charging. (The image contrast also disappears when the surface is coated with carbon (Fig. 9b), thus eliminating the possibility that the contrast is obscured by scattered electrons from the gold coating.)

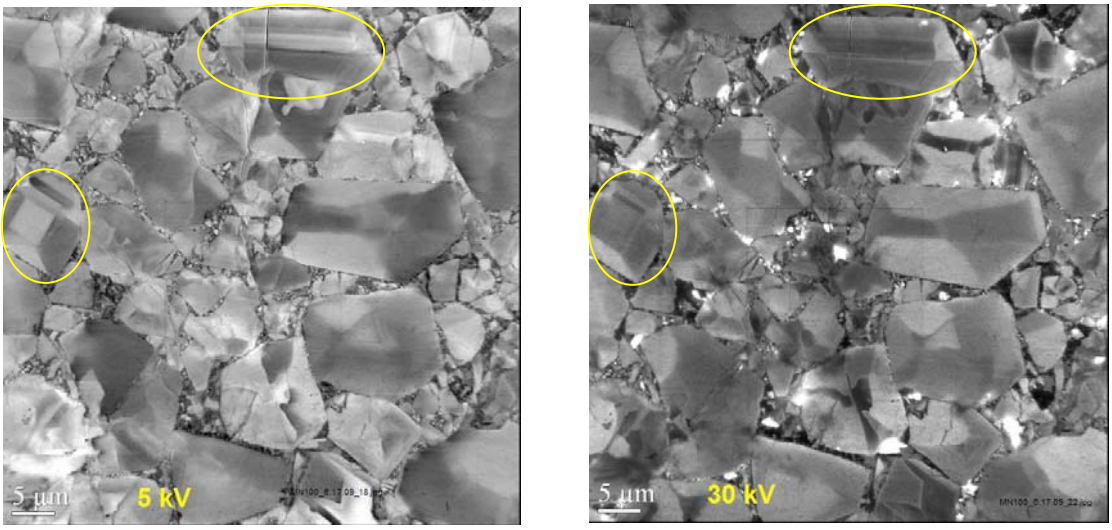

Fig. 8. Reversal of contrast in secondary electron images from uncoated surface of MN100 material at two different accelerating voltages: (a) 5 KV; (b) 30 KV.

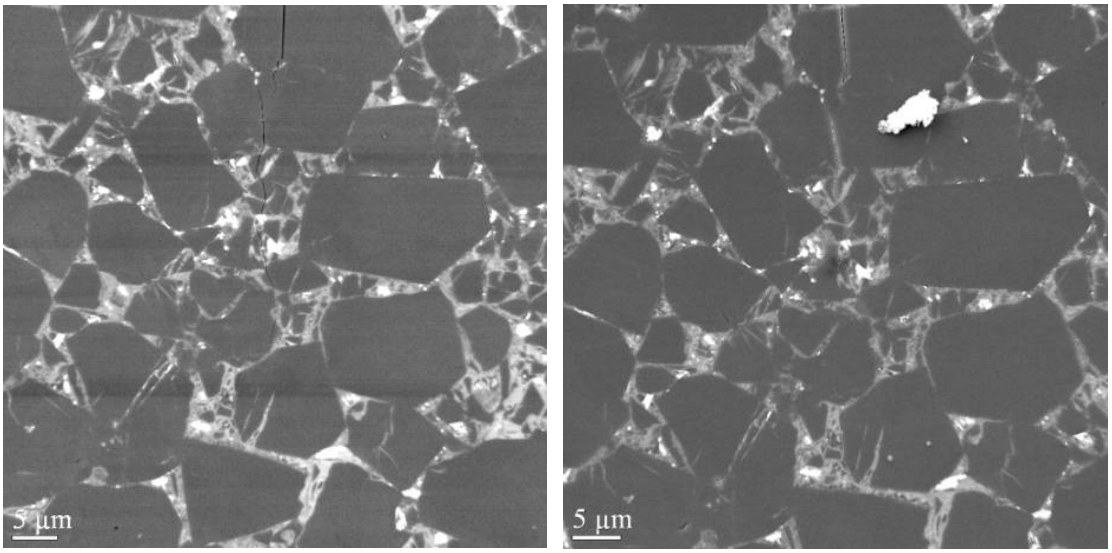

Fig. 9. Images from area of Fig. 8: (a) backscattered electron image, uncoated surface; (b) secondary electron image after coating the surface with carbon.

We hypothesize that these contrast features may correspond to internal twins or other deformation structures in BN grains, possibly caused local contact forces due to grain-to-grain contact during high pressure consolidation. Similar contrast features are observed in the MS80 materials, although only a small fraction of grains show internal features (consistent with expectation that, with the higher binder content, less damage occurs in MS80 from neighboring grains being in direct contact during densification).

Fracture Mechanisms in PCBN

The questions we seek to answer through fractography and controlled experiments include the following:
- Which is more important for tool life, initiation of periodic cracks, growth of periodic cracks, instability condition, or further growth of large cracks?
- Relation of cracking to microstructure? Are cracks always located in the intergranular phase?
- How do various stages of crack growth relate to known stress fields and material properties? Can we develop a fracture mechanics analysis that captures the various stages of growth?
- Is the mechanism of cracking monotonic growth or cyclic fatigue?
- Implications for tool design?

Several PCBN tools with varying degrees of damage from FSW experiments have been removed from the tool holders for sectioning and fractography.

(i) Tool with relatively minor cracking

Photos of the top and bottom of the tool are shown in Fig. 10. Several cracks oriented in radial directions are visible on the top surface. One of these (A-B) was continuous around the sides and bottom of the tool insert. The others were continuous around the sides but either ended or followed more irregular paths on the bottom.

The PCBN tool rested on a WC/Co insert in the holder. The top of this insert had ridges that mirrored the pattern of cracks on the bottom of the PCBN tool (Fig. 10).

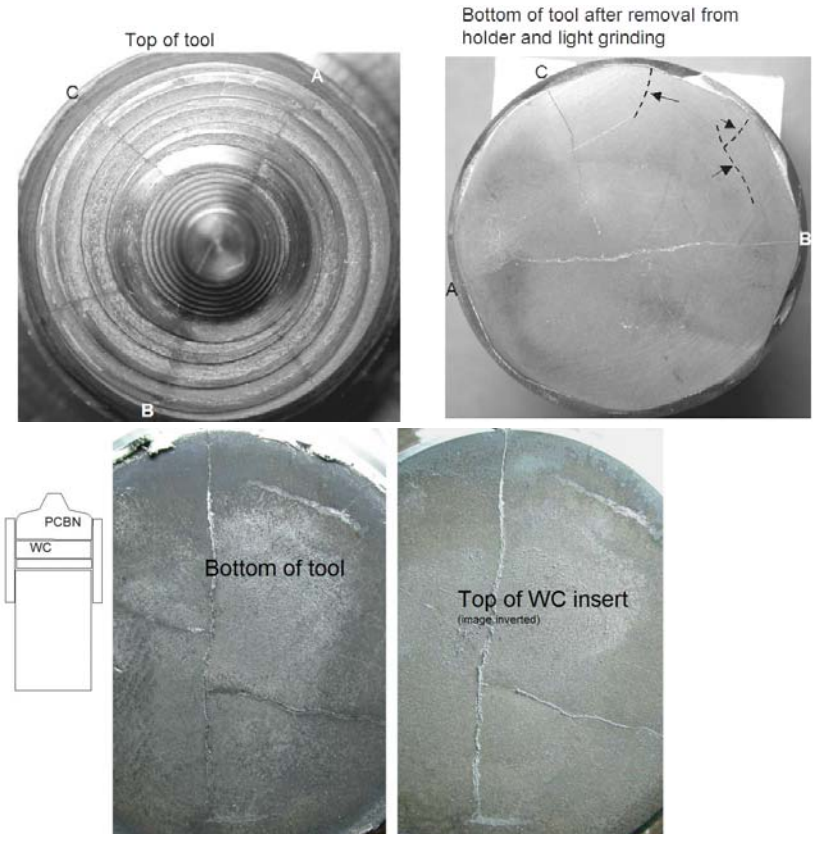

Fig. 10. Top and bottom surfaces of PCBN tool and top surface of WC/Co insert after removal from holder.

SEM analysis of the WC/Co insert after sectioning indicated that the ridges corresponds to an underlying reaction zone consisting of regions of Co-Al metal and regions with WC particles in a metal of similar composition. Examination of the bottom of the PCBN tool indicated that most cracks were filled, at least near the surface, with metal consisting of regions of C-containing Al surrounding regions of Al-W-Co (Fig. 11). In some regions it appeared that this material had chipped out when the tool was removed leaving an underlying region containing Al., Zr,O,W and Co. The presence of Zr and O is accounted for by a spray coating of ZrO_2 that was applied to the tool surface before assembly. The only potential source of Al metal is the decomposition of trace amounts of AlB_2 formed in the PCBN material during its densification:

$$AlB_2 \rightarrow AlB_{12} + Al, \qquad (T > 980^oC)$$

This reaction indicates that the temperature at the base of the PCBN tool exceeded ~1000^{o}C during use. At this temperature, an Al liquid phase can contain up to ~10% Co, consistent with the observed reaction of the Al with the Co grain boundary phase in the WC/Co insert.

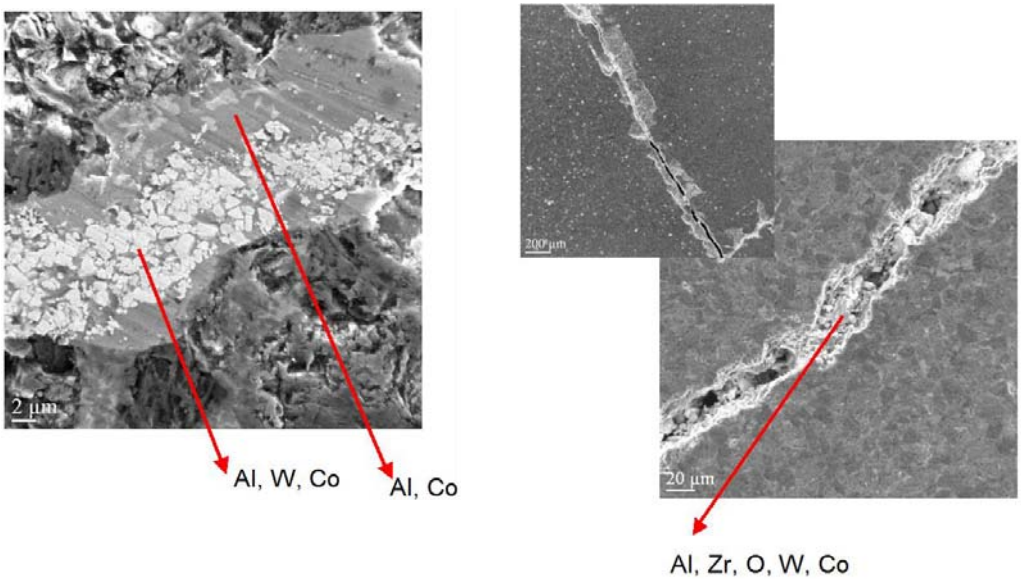

Fig. 11. SEM analysis of material filling cracks in the bottom of the PCBN tool from Fig. 10

The PCBN tool in Fig 10 was broken apart along crack A-B, as indicated in Fig. 12, after infiltrating the cracks with a dye penetrant. A large force (1200 N) was required to fracture the tool. The force was large for two reasons: (i) although the crack A-B formed a closed path around the outside of the tool, there were intact regions in the interior, near the top of the tool, where the crack had not penetrated (visible in Fig. 12 as gray regions that were not decorated by the pink dye penetrant); (ii) large areas of the cracked region were strongly bonded together with Al metal, as indicated in subsequent SEM analysis, which showed the ductile rupture of Al metal on both sides of matching fracture surfaces (Fig. 13).

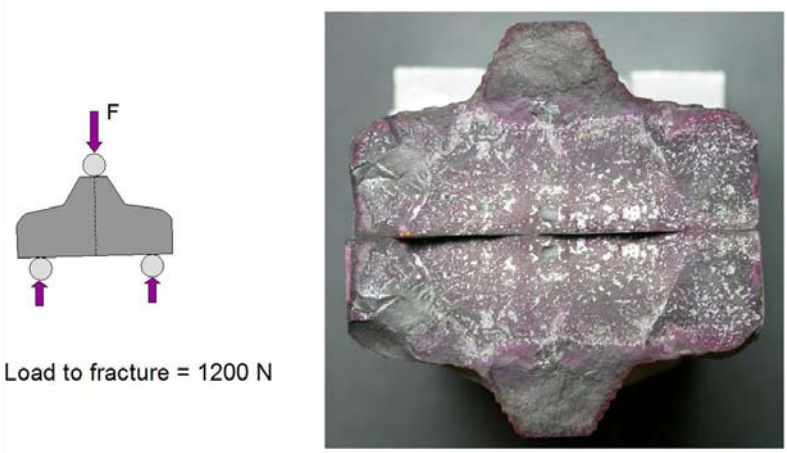

Fig. 12. Fracture of the PCBN tool from Fig. 10 along crack A-B

The composition of the metal that filled most of the cracked region varied with location. Near the top of the tool there was a large amount of Fe and Al, the Fe coming from the steel work piece that was used in the FSW and the Al from the decomposition reaction mentioned above. Near the bottom of the tool the metal was mostly Al, with a trace of Fe in local regions.

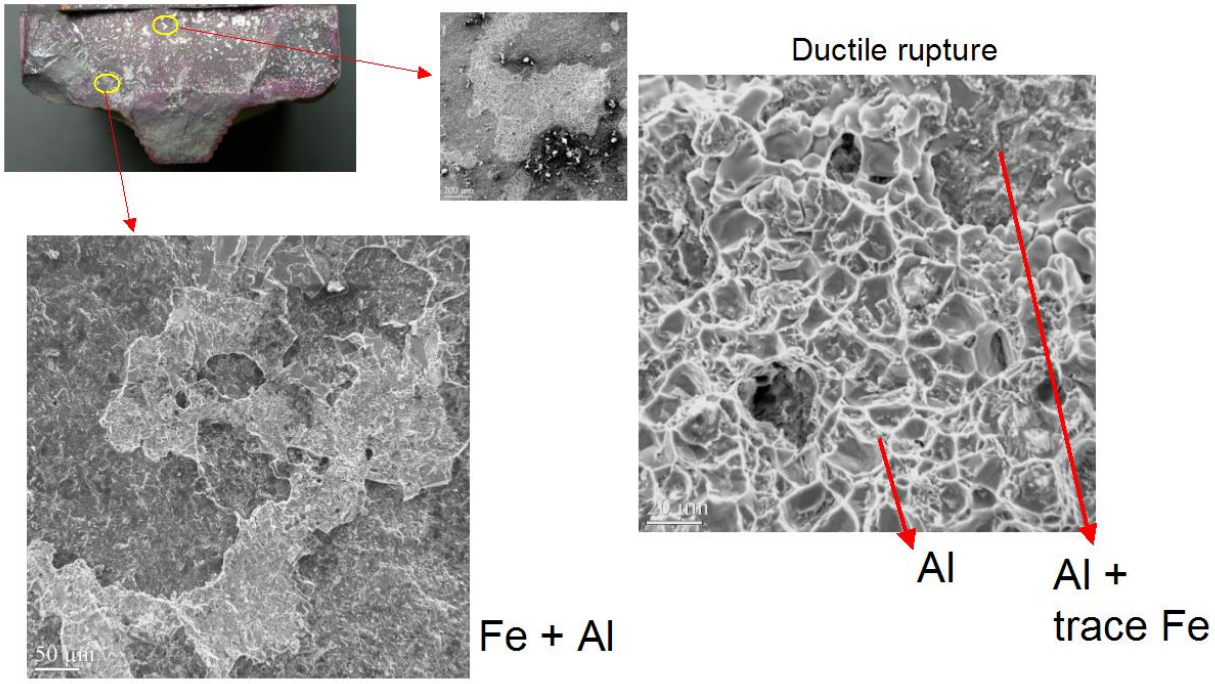

Fig. 13. SEM analysis of fracture surface of tool in Fig. 12

In summary, these observations indicate that there were at least 6 major cracks in the tool, none of which passed completely through tool. This explains the general observation that these types of tools continue to function surprisingly well in FSW long after they are severely cracked. The observations indicate that crack growth occurs incrementally, likely over many thermal and/or mechanical cycles, rather than by

unstable growth at a critical condition. The presence of Al liquid filling the cracks indicates that the temperature exceeded ~1,000^{o}C throughout the PCBN tool during FSW. Under these conditions diffusion of Fe from work piece occurred into the Al liquid in cracks through most of tool thickness.